

How Many Antimicrobial Peptide Molecules Kill a Bacterium? The Case of PMAP-23

Daniela Roversi,[†] Vincenzo Luca,[‡] Simone Aureli,[†] Yoonkyung Park,[§] Maria Luisa Mangoni,[‡] and Lorenzo Stella^{*†}

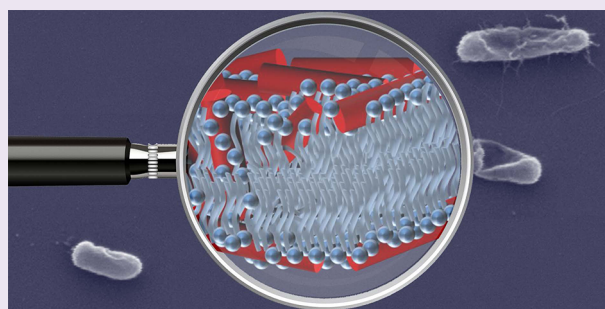
[†]Department of Chemical Sciences and Technologies, University of Rome Tor Vergata, 00133 Rome, Italy

[‡]Department of Biochemical Sciences "A. Rossi Fanelli", Istituto Pasteur-Fondazione Cenci Bolognetti, Sapienza Rome University, 00185 Rome, Italy

[§]Department of Biotechnology, Chosun University, 501-759 Gwangju, Korea

S Supporting Information

ABSTRACT: Antimicrobial peptides (AMPs) kill bacteria mainly through the perturbation of their membranes and are promising compounds to fight drug resistance. Models of the mechanism of AMPs-induced membrane perturbation were developed based on experiments in liposomes, but their relevance for bacterial killing is debated. We determined the association of an analogue of the AMP PMAP-23 to *Escherichia coli* cells, under the same experimental conditions used to measure bactericidal activity. Killing took place only when bound peptides completely saturated bacterial membranes (10^6 – 10^7 bound peptides per cell), indicating that the "carpet" model for the perturbation of artificial bilayers is representative of what happens in real bacteria. This finding supports the view that, at least for this peptide, a microbicidal mechanism is possible *in vivo* only at micromolar total peptide concentrations. We also showed that, notwithstanding their simplicity, liposomes represent a reliable model to characterize AMPs partition in bacterial membranes.



Antimicrobial peptides (AMPs) constitute a first defense against pathogens.¹ In addition to other functions, they are broad spectrum bactericidals, which usually act by perturbing the permeability of bacterial membranes.² This mechanism of action makes the development of bacterial resistance particularly unlikely,³ and therefore these peptides are investigated as lead compounds to fight multiple drug-resistant bacteria,⁴ a dramatic and increasing threat.⁵ However, in order to develop new molecules with the same activity as AMPs, but with better drug-like properties, it is essential to fully understand their mechanism of bacterial killing.⁴

Several models of pore formation by AMPs have been proposed,^{6–8} but they are all based on biophysicochemical studies on artificial vesicles. Therefore, their relevance to what actually happens in real bacteria is a topic of heated debate,⁹ with some authors claiming that results obtained in liposomes can be quantitatively extrapolated to microbiological experiments,^{10,11} and others reporting a total lack of correlation between the two data sets.¹² A related question is whether peptide concentrations *in vivo* are high enough to perturb the permeability of bacterial membranes.¹³ *In vitro* microbiological studies determine the lowest AMP concentration that inhibits bacterial growth (minimum inhibitory concentration, or MIC) or that causes a reduction in the number of viable bacteria $\geq 99.9\%$ (minimum bactericidal concentration, or MBC¹⁴). However, these values strongly depend on the conditions of the

assay.¹⁵ The real critical parameter, independent of experimental conditions, is not the total peptide concentration in the assay ($[P]_{\text{tot}}$), but the minimum number of peptide molecules that must bind to a bacterium to cause its death. However, guesses of this value extrapolated from water–membrane partition constants determined in liposome studies differ by more than 3 orders of magnitude.^{6,10}

Trying to fill the gap between biological and physicochemical studies, we determined experimental conditions that allow both the determination of microbicidal activity and the measurement of peptide/membrane association directly in bacteria. As a test case, we chose *E. coli* cells and the antimicrobial peptide PMAP-23, which we had previously extensively characterized.¹⁶ This peptide belongs to the cathelicidin family, is 23 residues long (RIIDLLWRVRRPQPKFVTWV), cationic, and amphipathic, and attains a helical conformation when membrane-bound. To determine peptide binding to bacterial cells, we used fluorescence spectroscopy, due to the high sensitivity of this technique.¹⁷ We ensured selective detection of the peptide signal by labeling PMAP-23 at the N-terminus with a dansyl (5-(dimethylamino)naphthalene-1-sulfonyl chloride) moiety, a

Received: May 28, 2014

Accepted: July 24, 2014

Published: July 24, 2014

Table 1. Membrane Coverage by D-PMAP-23 under the Conditions of the Bactericidal Assay

[D-PMAP-23] (μM)	fraction of surviving bacteria ^a	fraction of peptide bound to bacteria ^b	peptide molecules bound to a single cell ^c	peptide-covered area/bacterial membrane area ^d	$[\text{P}]_{\text{bound}}/[\text{L}]^e$	$[\text{P}]_{\text{bound}}/[\text{L}]$ (geometrical estimate) ^f
1.0	0.94 ± 0.03	0.89 ± 0.08	$(1.2 \pm 0.2) \times 10^6$	0.2	1:30	1:40
10	$(5 \pm 7) \times 10^{-4}$	0.829 ± 0.003	$(11 \pm 1) \times 10^6$	2	1:4	1:4

^aDetermined as the fraction of colony forming units (CFU) in a sample incubated for 2 h with different peptide concentrations, as compared with the CFU of the control at time zero, i.e., $(4.5 \pm 0.5) \times 10^8$ CFU/mL. ^bDetermined at a cell density of $(4.5 \pm 0.5) \times 10^8$ CFU/mL, from the data in Figure 1. ^cCalculated from the peptide and cell concentration and the fraction of bound peptide. ^dRatio between the area covered by the bound peptides and the total area of the inner and outer bacterial membranes (both leaflets). The reported values were calculated from the number of bound peptides per cell, assuming that each *E. coli* cell corresponds to a cylinder of 1 μm diameter and 2 μm height,²² and an area per D-PMAP-23 molecule of $(5.4 \pm 0.6) \text{ nm}^2$. ^eRatio between the number of bound peptides and the number of lipids in a bacterial cell, calculated by assuming that each cell contains roughly 4×10^7 lipids (see Methods). ^fRatio between the number of bound peptides and the number of lipids in a bacterial cell, calculated by assuming that each *E. coli* cell corresponds to a cylinder of 1 μm diameter and 2 μm height,²² with four membrane leaflets, and an area per lipid of 0.7 nm^2 .^{6,10,18,22} This corresponds to 4.5×10^7 lipids per cell. Values representing just order of magnitude estimates are reported with 1 significant digit and with no error. Further details concerning these calculations are reported in the Methods.

probe extremely sensitive to the environment polarity that can be excited at wavelengths where intrinsic fluorophores do not absorb.¹⁸ Labeling slightly affected peptide activity, causing an increase in the MIC by a factor of 2 (data not shown). In any case, all experiments were performed with the labeled analogue (D-PMAP-23) and are thus directly comparable.

The antibacterial activity of AMPs is usually assessed by determining the MIC, but this assay was not suitable for our purposes. By definition, the MIC assay requires a medium in which bacteria grow, while we needed a well-defined and stable cell density. In addition, we observed that MIC values strongly depended on the concentration of the culture broth (Mueller–Hinton broth, MH), as already reported in the literature,¹⁹ a finding indicating peptide sequestration by medium components. Finally, the MH medium is colored and fluorescent in the visible region,²⁰ and therefore it could interfere with dansyl fluorescence. For all these reasons, in this study we used bacterial killing (rather than growth inhibition) measurements and identified a minimal culture medium (5 mM HEPES, pH 7.3, 110 mM KCl, 15 mM glucose) where bacteria remain vital but do not multiply, maintaining a constant number of live cells for several hours (Supplementary Figure 1). The bacterial killing assay performed in the presence of $(4.5 \pm 0.5) \times 10^8$ cells/mL at 37 °C showed that the bactericidal activity of D-PMAP-23 starts at $[\text{P}]_{\text{tot}} = 1.0 \mu\text{M}$, and total bacterial killing is attained at $[\text{P}]_{\text{tot}} = 10 \mu\text{M}$ (Table 1 and Supplementary Figure 2). Therefore, we selected these two peptide concentration values for the association experiments.

We performed experiments of peptide binding to bacterial membranes under the same conditions (temperature and medium) of the biological assay. When D-PMAP-23 was titrated with increasing concentrations of *E. coli* cells, its emission spectrum exhibited an increase of the fluorescence intensity and a blue shift of the maximum (Figure 1a). These are distinctive features of dansyl insertion in an apolar, relatively rigid environment and thus indicate association to bacterial membranes. We checked for possible effects of sample turbidity (caused by the bacterial cells in suspension) on the spectroscopic signal, by control measurement performed with fluorophores not expected to bind to bacteria, i.e., the dansyl analogue dansylamide and dextrans labeled with coumarin or rhodamine. In these cases, titration with bacterial cells did not cause significant variations in the fluorescent signal (Supplementary Figure 3), demonstrating the absence of any relevant scattering-related artifacts.^{17,21} This conclusion was confirmed also by following peptide/bacteria association through

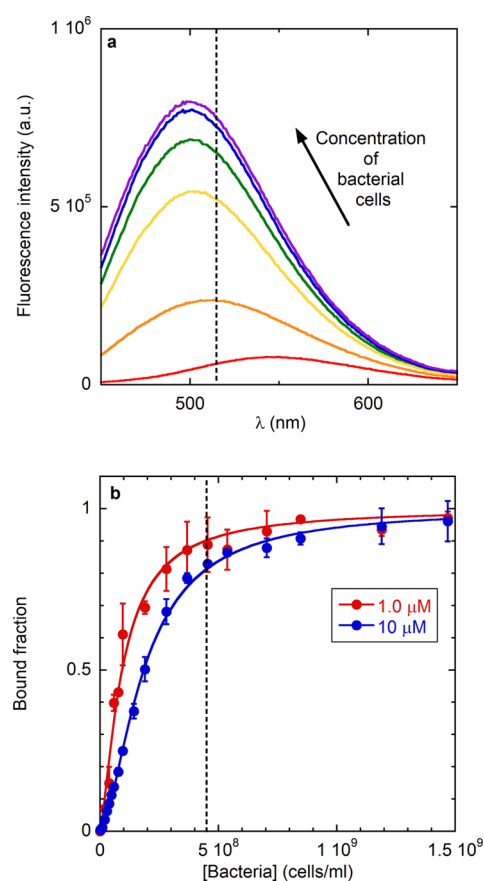


Figure 1. Fluorimetric determination of peptide binding to bacterial cells. (a) Fluorescence spectra of D-PMAP-23 (10 μM) in the presence of increasing *E. coli* cell densities (0, 9.6×10^7 , 2.8×10^8 , 4.5×10^8 , 8.4×10^8 , 1.5×10^9 cells/mL). Spectra are colored from red to violet with increasing cell concentration. Emission intensity at $\lambda = 515$ nm (corresponding to the vertical dashed line) was used to calculate the fraction of bound peptide reported in panel b. (b) Fraction of D-PMAP-23 bound to bacterial cells. Blue symbols: [D-PMAP-23] = 1.0 μM . Red symbols: [D-PMAP-23] = 10 μM . The continuous lines represent a guide for the eye. Error bars indicate the range of duplicate measurements. The vertical dashed line corresponds to the concentration of 4.5×10^8 cells/mL used in the bacterial killing experiments.

variations in the dansyl fluorescence time-decay, which is not affected by scattering (Supplementary Figure 4). We calculated the fraction of peptide bound to bacterial membranes from the

variation of fluorescence intensity at a fixed wavelength (515 nm) (Figure 1b). The bound fraction depended on $[P]_{\text{tot}}$ and deviated from a strictly hyperbolic dependence on the density of bacterial cells, indicating a slight departure from the behavior expected for a perfectly ideal partition between two phases.^{10,11}

The data in Figure 1 provided the answer to the question in our title, since it allowed us to calculate the number of peptide molecules bound to bacterial cells (Table 1): $(1.2 \pm 0.2) \times 10^6$ bound peptide molecules per cell at $[P]_{\text{tot}} = 1.0 \mu\text{M}$, i.e., where bacterial killing starts, and $(11 \pm 1) \times 10^6$ at $[P]_{\text{tot}} = 10 \mu\text{M}$, i.e., at a concentration causing the death of all bacteria in the sample. To understand the implication of these numbers, it should be considered that a single bound peptide molecule covers an area of at least 5 nm^2 and that the total area of all *E. coli* membranes (i.e., both leaflets of the outer and inner membranes of this Gram-negative bacterium) is about $3 \times 10^7 \text{ nm}^2$ (see Methods). Therefore, the numbers of bound peptides determined in our experiments correspond to an extremely high coverage of the bacterial membranes, with the effective area of the bound peptides even exceeding the total membrane area at $[P]_{\text{tot}} = 10 \mu\text{M}$ (Table 1). This last finding could be due to the approximations involved in our estimates, but it might also indicate a multilayer arrangement of the peptides or peptide association to bacterial components different from lipids, such as the polysaccharide chains of the outer leaflet of the outer membrane or membrane proteins. However, it should be noted that the increase in fluorescence intensity observed at 515 nm in our assay was accompanied by a shift of the spectrum to shorter wavelengths and thus to insertion of the probe into an apolar, membrane-like environment. Indeed, the spectral shift observed with bacteria was the same caused by association to phospholipid vesicles (see below and Supplementary Figure 5).

A high membrane coverage is usually needed also to perturb the permeability of artificial membranes.¹⁰ One of the mechanisms of pore formation hypothesized on the basis of physicochemical studies on model systems is the so-called "carpet" model, where destabilization of phospholipid bilayers is caused by peptide accumulation on their surface.^{6,7,22} We previously demonstrated that this model holds also for PMAP-23 in artificial membranes.^{7,16} The present data suggest that the carpet model is representative also of what is actually happening in real bacteria.

Liposomes are generally the best model systems to characterize AMPs/membrane interactions, but it is debated whether results obtained with vesicles are relevant for peptide behavior in bacteria.¹² To directly compare our findings with bacterial cells with those in model membranes, we estimated that the number of lipids in a single *E. coli* cell is roughly 4×10^7 (see Methods). On the basis of this value, we could assess that bacterial killing starts at a molar ratio of bound peptide per lipid ($[P]_{\text{bound}}/[L]$) of about 1:30, and that all bacteria are killed when this value arrives at 1:4 (Table 1). We reached a similar conclusion also by a completely different approach, based on the total membrane area of a bacterial cell (Table 1 and Methods),^{6,11,19,23} confirming the validity of this order of magnitude assessment. The $[P]_{\text{bound}}/[L]$ values determined here in bacteria are extremely similar to those estimated by Castanho and co-workers for other peptides, based on the partition constants derived from binding studies on model membranes.¹⁰ In addition, they are also comparable to the threshold values needed to cause liposome leakage.¹⁰ This prompted us to compare directly D-PMAP-23 binding to

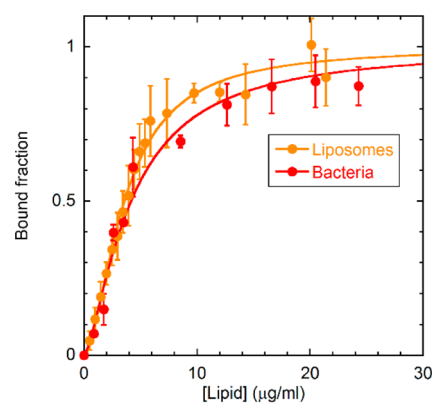


Figure 2. Comparison of peptide binding to bacteria and artificial membranes. Fraction of D-PMAP-23 ($1.0 \mu\text{M}$) bound to *E. coli* cells (red symbols) and to liposomes composed of lipids extracted from *E. coli* (orange symbols). The continuous lines represent a guide for the eye. Error bars indicate the range of duplicate measurements. Lipid concentrations in experiments with bacteria were estimated by considering that each cell contains 45 fg of lipids (see Methods).

bacteria and to liposomes composed of *E. coli* lipid extract, under the same experimental conditions (Supplementary Figure 5). In Figure 2 we report the two binding isotherms, as a function of total lipid concentration. The two curves are surprisingly similar, indicating that, despite their simplicity, liposomes are a good model to study peptide association to bacterial lipids.

Concentrations of bacteria in infected areas can be comparable to those used in our assay,²⁴ and therefore the results presented here show that local micromolar concentrations of AMPs are needed for effective bacterial killing. However, our data allow us to calculate the number of peptide molecules bound to each bacterial cell, as a function of the bacterial concentration (Supplementary Figure 6). These data indicate that, even at much lower cell densities, $[D\text{-PMAP-23}]_{\text{tot}}$ values in the low micromolar range would still be needed to reach the threshold necessary to kill bacteria. This finding supports the hypothesis that *in vivo* a microbicidal mechanism is possible only where endogenous AMPs reach these relatively high concentrations,²⁵ and that therefore their immunomodulatory activity might prevail in other cases.²⁶

In summary, we determined that PMAP-23 must completely saturate bacterial membranes to cause cell death and showed that binding isotherms obtained in bacteria and in model membranes are comparable. These findings support the relevance of the carpet model of membrane perturbation for the mechanism of bacterial killing. Finally, our data indicate that micromolar values of $[P]_{\text{tot}}$ are needed for effective bactericidal activity and therefore suggest that other functions might prevail where these relatively high peptide concentrations cannot be reached. Considering that several AMPs have very similar active concentrations and membrane affinities,¹⁰ our findings might be relevant also to other peptides.

METHODS

Materials. *E. coli* extracted lipids were purchased from Avanti Polar Lipids (Alabaster, AL, Canada). 5-(Dimethylamino)-1-naphthalenesulfonamide (dansylamide), 7-amino-4-methylcoumarin-labeled dextran (40 kDa), and rhodamine B isothiocyanate-labeled dextran (10 kDa) were purchased from Sigma-Aldrich (St. Louis, MO, USA). Spectroscopic-grade chloroform and methanol (Carlo Erba, Milano, Italy) were used. PMAP-23 and the D-PMAP-23 analogue, labeled

with 5-(dimethylamino)naphthalene-1-sulfonyl (dansyl) at the N-terminus and amidated at the C-terminus, were purchased from AnyGen Co. (Gwangju, South Korea). Bacterial culture media were purchased from Oxoid (Basingstoke, U.K.), and 96-well plates were from Falcon (Franklin Lakes, NJ, USA).

Bactericidal Activity. *E. coli* ATCC 25922 was grown in Luria–Bertani (LB) medium at 37 °C in an orbital shaker until a mid-log phase, which was aseptically monitored by absorbance at 590 nm ($A_{590\text{ nm}} = 0.8$) with an UV-1700 Pharma Spec spectrophotometer (Shimadzu, Tokyo, Japan). Afterward, bacterial cells were centrifuged ($1.4 \times g$ for 10 min) and washed eight times in buffer A (5 mM HEPES, pH 7.3, 110 mM KCl, 15 mM glucose) to remove traces of LB medium. This buffer was selected by analogy to those used in fluorescence assays of bacterial membrane depolarization.²⁷ Bacteria cells, suspended in buffer A [$(4.5 \pm 0.5) \times 10^7$ CFU], were added to different concentrations of D-PMAP-23 (final volume of 100 μ L) or to methanol (the peptide solvent) for the control. Samples were then incubated at 37 °C and 800 rpm in an Eppendorf Thermomixer Comfort (Eppendorf s.r.l., Milan, Italy). After 120 min (30, 60, and 120 min for the control), aliquots of 5 μ L were withdrawn, diluted in buffer A, and spread onto LB-agar plates for counting after overnight incubation at 37 °C. Survival of bacterial cells at different time intervals was expressed as percentage with respect to the initial number (time zero).^{14,28} All data are the mean of three independent experiments \pm SD.

Liposome Preparation. Large unilamellar vesicles (100 nm diameter), formed by *E. coli* extracted lipids, were prepared as previously described.²⁹ The final lipid concentration was determined by the Stewart method.³⁰

Peptide Association to Bacteria and Liposomes. Bacterial cells were grown, collected, and washed as described above and resuspended in buffer A at a final cell density of 6×10^9 CFU/mL. Experiments were performed on the same day. Measurement samples were maintained at 37 °C, while stock cell suspensions were at 25 °C. As indicated by colony counts at different times (Supplementary Figure 1), these conditions ensured a stable number of vital cells for at least 6 h at 25 °C or 2 h at 37 °C (i.e., more than the time required for our experiments under those conditions).

A fixed peptide concentration (in buffer A) was titrated with increasing concentrations of bacterial cells or liposomes. After each addition, the fluorescence spectra were recorded repeatedly until no further changes were observed (about 5–10 min).

Experiments were performed with a HORIBA (Edison, NJ) FluoroMax-4 fluorimeter, with $\lambda_{\text{exc}} = 340$ nm, integration time 0.4 s, bandwidths of 1.5–2 nm in excitation and emission, respectively, when a peptide concentration of 10 μ M was used, or 2.5–3 nm for a peptide concentration of 1 μ M. The temperature was controlled with a thermostated cuvette holder set at 37 °C for all experiments.

Control experiments to check for possible effects of sample turbidity on the fluorescence signal were performed by repeating the same titration (using the same conditions of the 10 μ M D-PMAP-23 experiments) with three different probes, dansylamide and dextrans labeled with coumarin or rhodamine.

The fraction of peptide associated with membranes was calculated from the fluorescence intensity at 515 nm (F), according to the following equation:

$$f = \frac{F - F_W}{F_M - F_W}$$

where F_W and F_M represent the fluorescence intensities of the peptide in water and in the membrane, respectively. The latter was determined by fitting directly the F vs [cells] titration with the following phenomenological Hill equation:

$$F = F_W + (F_M - F_W) \frac{(K[\text{Cells}])^n}{1 + (K[\text{Cells}])^n}$$

where K represents an apparent dissociation constant, [cells] is the concentration of bacterial cells, and n is a parameter to take into account the sigmoidal shape of the curve.

The time decays of peptide fluorescence ($[D\text{-PMAP-23}] = 20 \mu\text{M}$) in the presence of different concentrations of bacterial cells were measured with a Lifespec-ps time-correlated single photon counting apparatus by Edinburgh instruments (Edinburgh, U.K.), with a NanoLed source (340 nm, 5 MHz repetition rate), and the whole emission spectrum was collected through two stacked cut-off filters (389 and 420 nm), by setting the monochromator to the 0th order of diffraction. Temperature was controlled to 37 °C by a thermostated cuvette holder. Fluorescence intensity decays were acquired until a peak value of 10^4 counts was reached and analyzed according to a triple exponential model. The fraction of peptide bound to bacterial membranes was calculated from the amplitude-weighted lifetime ($\langle\tau\rangle$) values,¹⁷ according to the following equation:

$$f = \frac{\langle\tau\rangle - \langle\tau\rangle_W}{\langle\tau\rangle_M - \langle\tau\rangle_W}$$

where $\langle\tau\rangle_W$ and $\langle\tau\rangle_M$ represent the values of $\langle\tau\rangle$ for the peptide in water and in the membrane, respectively.

Calculations of Molar and Area Ratios. The fraction of membrane area covered by bound peptides was estimated by assuming a cylindrical shape for an *E. coli* cell, with a diameter of 1 μm and a length of 2 μm .²³ In order to take into consideration the maximum available area, both leaflets of the two membranes of Gram-negative bacteria were considered, in agreement with the previously demonstrated ability of PMAP-23 and other AMPs to reach and permeabilize the inner membrane.^{31,32} The area covered by a single bound peptide molecule was assessed by considering that previous molecular dynamics simulations of PMAP-23 in membranes⁷ indicated that each peptide molecule occupies an area corresponding to 9 ± 1 lipids. Since in that system each lipid occupied an area of about 0.6 nm^2 , this corresponds to $5.4 \pm 0.6 \text{ nm}^2$. This estimate was comparable to values obtained by other methods, such as approximating the shape of the helical peptide to a cylinder.

The number of lipids per cell was estimated in two ways:

1. According to ref 11, by considering that each dry *E. coli* cell weights 489 fg³³ and that 9.2% of this is formed by lipids,³⁴ yielding a lipid content of 45 fg per cell (this value was used to convert cell densities to lipid concentrations in Figure 2). Assuming an average lipid molecular weight of 692 Da,¹¹ this corresponds to a number of lipids per cell of about 4×10^7 .

2. According to refs 6 and 19, by considering the total area of the membranes of a single *E. coli* cell (see above) and an average area per lipid of 0.7 nm^2 .³⁵ This corresponds to a number of lipids per cell of about 4.5×10^7 .

Both methods yielded comparable results (Table 1).

It should be noted that the outer leaflet of the outer membrane of Gram-negative bacteria contains lipopolysaccharide (LPS) molecules and that each of them usually has 6 acyl chains, compared to the 2 chains of phospholipids. However, LPS also has an area per molecule corresponding to about 3 phospholipids.¹⁹ In our calculations (which, in any case, are just order of magnitude estimates), an LPS molecule is essentially counted as 3 phospholipid molecules.

■ ASSOCIATED CONTENT

📄 Supporting Information

This material is available free of charge via the Internet at <http://pubs.acs.org>.

■ AUTHOR INFORMATION

Corresponding Author

*E-mail: stella@stc.uniroma2.it.

Notes

The authors declare no competing financial interest.

■ ACKNOWLEDGMENTS

We thank G. Bocchinfuso and A. Farrotti for stimulating discussions and help with the graphical abstract. This research

was supported by the Italian Ministry of Education, University and Research (grant 2010NRREPL_008, to L.S.) and National Research Foundation of Korea (grant 2011-0017532, to Y.P.).

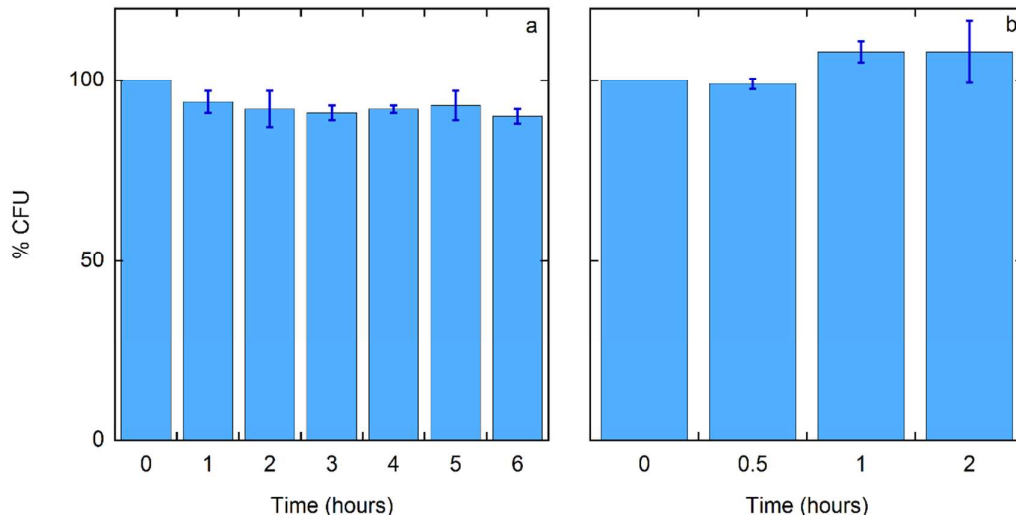
REFERENCES

- (1) Hancock, R. E. W., and Sahl, H. G. (2006) Antimicrobial and host-defense peptides as new anti-infective therapeutic strategies. *Nat. Biotechnol.* 12, 1551–1557.
- (2) Peters, B. M., Shirliff, M. E., and Jabra-Rizk, M. A. (2010) Antimicrobial peptides: primeval molecules or future drugs? *PLoS Pathog.* 6, e1001067.
- (3) Peschel, A., and Sahl, H. G. (2006) The co-evolution of host cationic antimicrobial peptides and microbial resistance. *Nat. Rev. Microbiol.* 4, 529–536.
- (4) Fox, J. C. (2013) Antimicrobial peptides stage a comeback. *Nat. Biotechnol.* 31, 379–382.
- (5) Arias, C. A., and Murray, B. E. (2009) Antibiotic-resistant bugs in 21st century- A clinical super-challenge. *N. Engl. J. Med.* 360, 439–443.
- (6) Wimley, W. C. (2010) Describing the mechanism of antimicrobial peptide action with the interfacial activity model. *ACS Chem. Biol.* 5, 905–917.
- (7) Bocchinfuso, G., Palleschi, A., Orioni, B., Grande, G., Formaggio, F., Toniolo, C., Park, Y., Hahm, K. S., and Stella, L. (2009) Different mechanism of action of antimicrobial peptides: insights from fluorescence spectroscopy experiments and molecular dynamic simulations. *J. Pept. Sci.* 15, 550–558.
- (8) Bechinger, B., and Lohner, K. (2006) Detergent-like actions of linear amphipathic cationic antimicrobial peptides. *Biochim. Biophys. Acta* 1758, 1529–1539.
- (9) Wimley, W. C., and Hristova, K. (2011) Antimicrobial peptides: successes, challenges and unanswered questions. *J. Membr. Biol.* 239, 27–34.
- (10) Melo, N. M., Ferre, R., and Castanho, M. A. R. B. (2009) Antimicrobial peptides: linking partition, activity and high membrane-bound concentrations. *Nat. Rev. Microbiol.* 7, 245–250.
- (11) Melo, N. M., Ferre, R., Feliu, L., Bardaji, E., Planas, M., and Castanho, M. A. R. B. (2011) Prediction of antibacterial activity from physicochemical properties of antimicrobial peptides. *PLoS One* 6, e28549.
- (12) He, J., Krauson, A. J., and Wimley, W. C. (2014) Toward the de novo design of antimicrobial peptides: lack of correlation between peptide permeabilization of lipid vesicles and antimicrobial, cytolytic, or cytotoxic activity in living cells. *Biopolymers* 102, 1–6.
- (13) Jenssen, H., Hamill, P., and Hancock, R. E. W. (2006) Peptide antimicrobial agents. *Clin. Microbiol. Rev.* 19, 491–511.
- (14) Luca, V., Stringaro, A., Colone, M., Pini, A., and Mangoni, M. L. (2013) Esculentin(1-21), an amphibian skin membrane-active peptide with potent activity on both planktonic and biofilm cells of the bacterial pathogen *Pseudomonas aeruginosa*. *Cell. Mol. Life Sci.* 70, 2773–2786.
- (15) Sánchez-Gómez, S., Lamata, M., Leiva, J., Blondelle, S. E., Jerala, R., Andrä, J., Brandenburg, K., Lohner, K., Moriyón, I., and Martínez-de-Tejada, G. (2008) Comparative analysis of selected methods for the assessment of antimicrobial and membrane-permeabilizing activity: a case study for lactoferricin derived peptides. *BMC Microbiol.* 8, 196.
- (16) Orioni, B., Bocchinfuso, G., Kim, J. Y., Palleschi, A., Grande, G., Bobone, S., Park, Y., Kim, J., Hahm, K. S., and Stella, L. (2009) Membrane perturbation by the antimicrobial peptide PMAP-23: A fluorescence and molecular dynamics study. *Biochim. Biophys. Acta* 1788, 1523–1533.
- (17) Bocchinfuso, G., Bobone, S., Palleschi, A., and Stella, L. (2011) Fluorescence spectroscopy and molecular dynamics simulations in studies on the mechanism of membrane destabilization by antimicrobial peptides. *Cell. Mol. Life Sci.* 68, 2281–2301.
- (18) Lakowicz, J. R. (2006) *Principles of Fluorescence Spectroscopy*, Springer, New York.
- (19) Tossi, A., Sandri, L., and Giangaspero, A. (2000) Amphipathic, α -helical antimicrobial peptides. *Biopolymers* 55, 4–30.
- (20) Galeazzi, L., Groppa, G., and Giunta, S. (1990) Mueller–Hinton broth undergoes visible oxidative color changes in the presence of peroxidase and hydrogen peroxide. *J. Clin. Microbiol.* 28, 2145–2147.
- (21) Ladokhin, A. S., Jayasinghe, S., and White, S. H. (2000) How to measure tryptophan fluorescence in membrane properly, and why bother? *Anal. Biochem.* 285, 235–245.
- (22) Gazit, E., Miller, I. R., Biggin, P. C., Sansom, M. S., and Shai, Y. (1996) Structure and orientation of the mammalian antibacterial peptide cecropin P1 within phospholipid membranes. *J. Mol. Biol.* 258, 860–870.
- (23) Schulz, H. N., and Jorgensen, B. B. (2001) Big bacteria. *Annu. Rev. Microbiol.* 55, 105–137.
- (24) König, C., Simmen, H. P., and Blaser, J. (1998) Bacterial concentrations in pus and infected peritoneal fluid—implications for bactericidal activity of antibiotics. *J. Antimicrob. Chemother.* 42, 227–232.
- (25) Ganz, T. (2003) Defensins: antimicrobial peptides of innate immunity. *Nat. Rev. Immunol.* 3, 710–720.
- (26) Hilchie, A. L., Wuerth, K., and Hancock, R. E. W. (2013) Immune modulation by multifaceted cationic host defense (antimicrobial) peptides. *Nat. Chem. Biol.* 9, 761–768.
- (27) Wu, M., Maier, E., Benz, R., and Hancock, R. E. W. (1999) Mechanism of interaction of different classes of cationic antimicrobial peptides with planar bilayers and with the cytoplasmic membrane of *Escherichia coli*. *Biochemistry* 38, 7235–7242.
- (28) Mangoni, M. L., Maisetta, G., Di Luca, M., Gaddi, L. M., Esin, S., Florio, W., Brancatisano, F. L., Barra, D., Campa, M., and Batoni, G. (2008) Comparative analysis of the bactericidal activities of amphibian peptide analogues. *Antimicrob. Agents Chemother.* 52, 85–91.
- (29) Bobone, S., Piazzon, A., Orioni, B., Pedersen, J. Z., Nan, Y. H., Hahm, K.-S., Shin, A. Y., and Stella, L. (2011) The thin line between cell-penetrating and antimicrobial peptides: the case of Pep-1 and Pep-1-K. *J. Pept. Sci.* 17, 335–341.
- (30) Stewart, J. (1980) Colorimetric determination of phospholipids with ammonium ferrioxalate. *Anal. Biochem.* 104, 10–14.
- (31) Kim, J. Y., Park, S. C., Yoon, M. Y., Hahm, K. S., and Park, Y. (2011) C-terminal amidation of PMAP-23: translocation to the inner membrane of Gram-negative bacteria. *Amino Acids* 40, 183–195.
- (32) Lehrer, R., Barton, A., and Ganz, T. (1988) Concurrent assessment of inner and outer membrane permeabilization and bacteriolysis in *E. coli* by multiple-wavelength spectrophotometry. *J. Immunol. Methods* 108, 153–158.
- (33) Loferer-Kröbber, M., Klima, J., and Psenner, R. (1998) Determination of bacterial cell dry mass by transmission electron microscopy and densitometric image analysis. *Appl. Environ. Microbiol.* 64, 688–694.
- (34) Kaneshiro, T., and Marr, A. G. (1962) Phospholipids of *Azotobacter agilis*, *Agrobacterium tumefaciens*, and *Escherichia coli*. *J. Lipid Res.* 3, 184–189.
- (35) Marsh, D. (1990) *Handbook of Lipid Bilayers*, CRC Press, Boca Raton.

Supporting Information for:

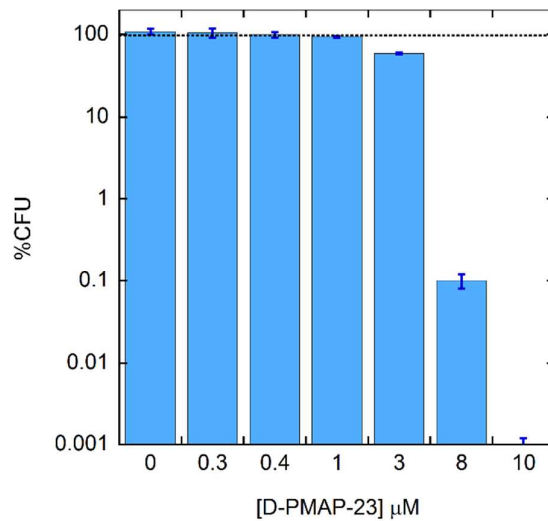
How many antimicrobial peptide molecules kill a bacterium? The case of PMAP-23

Daniela Roversi, Vincenzo Luca, Simone Aureli, Yoonkyung Park, Maria Luisa Mangoni and
Lorenzo Stella



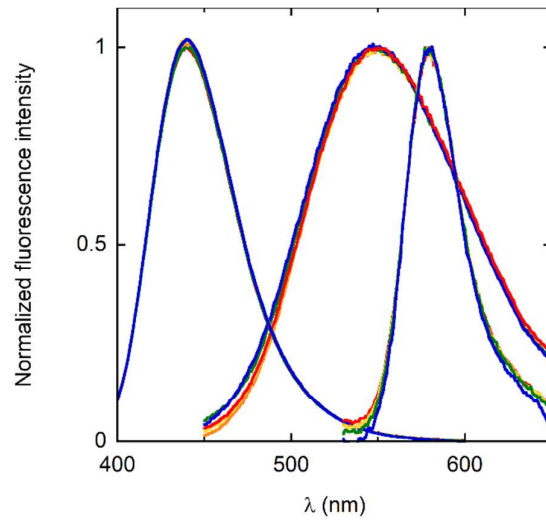
Supplementary Figure 1 Survival of *E. coli* cells in the minimal medium

Percentage of viable *E. coli* after resuspension in buffer A, as a function of time. Temperature and starting cell density were set at 25 °C, $6 \cdot 10^9$ CFU/ml (panel a) and 37 °C, $4.5 \cdot 10^8$ CFU/ml (panel b).



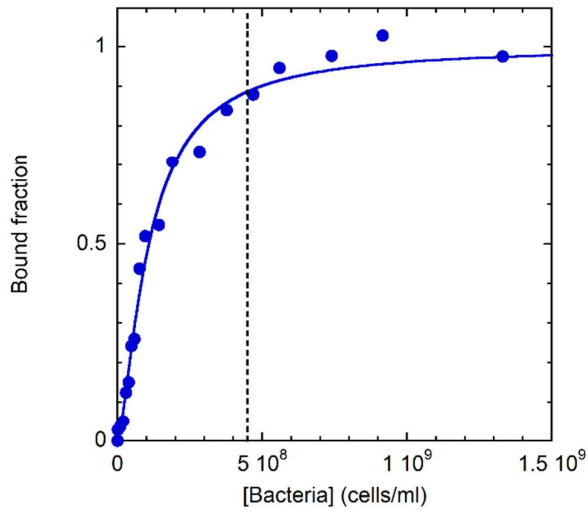
Supplementary Figure 2 Microbicidal activity of D-PMAP-23 on *E. coli* cells

Survival of *E. coli* cells ($4.5 \cdot 10^8$ CFU/ml) after 2h of incubation with different concentrations of D-PMAP-23 (37 °C).



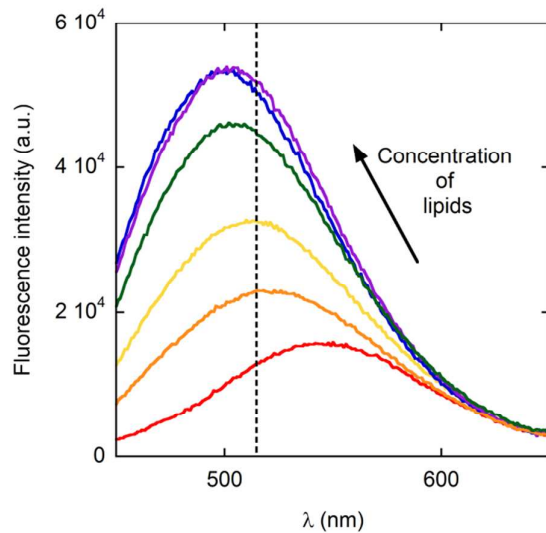
Supplementary Figure 3 Control experiments for possible light-scattering artefacts

Fluorescence spectra of coumarine-labeled dextran (left), dansylamide (middle) and rhodamine-labeled dextran (right) in the presence of increasing *E. coli* cell concentrations ($9.6 \cdot 10^7$, $2.8 \cdot 10^8$, $4.5 \cdot 10^8$, $8.4 \cdot 10^8$ cells/ml, colored from blue to red).



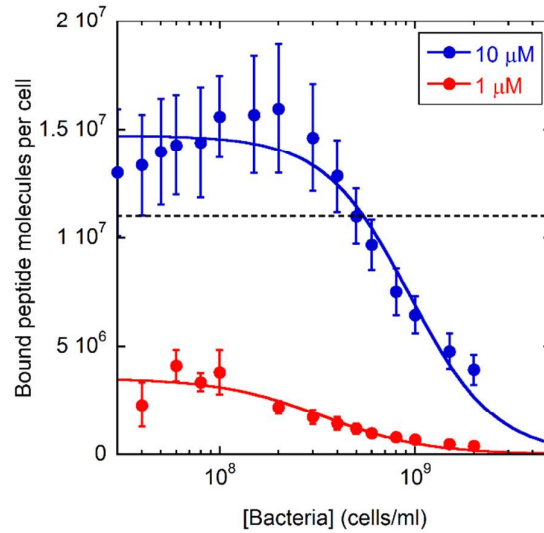
Supplementary Figure 4 Time-resolved measurements of D-PMAP-23 binding to bacteria

Fraction of D-PMAP-23 bound to *E.coli* cells calculated from time-resolved measurements ($[D\text{-PMAP-23}] = 20 \mu\text{M}$). The continuous line represents a guide for the eye. The vertical dashed line corresponds to the concentration of 4.5×10^8 cells/ml used in the bacterial killing experiments.



Supplementary Figure 5 Fluorimetric determination of peptide binding to liposomes.

Fluorescence spectra of D-PMAP-23 (10 μ M) in the presence of increasing liposome concentrations (0, 1.5, 3, 5, 10, 20 μ g/ml lipids). Spectra are colored from red to violet with increasing lipid concentration. Emission intensity at $\lambda=515$ nm (corresponding to the vertical dashed line) was used to calculate the fraction of bound peptide reported in Figure 2 of the main article.



Supplementary Figure 6 Bound peptide molecules per cell as a function of bacterial cell density

The number of bound peptide molecules per cell was calculated from the data in Figure 1b of the main text. The horizontal line represents the 1.1×10^7 threshold needed for total killing of bacteria.

Error bars indicate maximum errors (*i.e.* the propagation of the range of duplicate measurements for the bound peptide fraction and of the error on the number of cells in the assay).